

SYSTEMATIC OPTIMIZATION-BASED SYNTHESIS OF HYBRID SEPARATION PROCESSES

Wolfgang Marquardt, Korbinian Kraemer, Andreas Harwardt
Aachener Verfahrenstechnik – Process Systems Engineering, Templergraben 55, 52056 Aachen, Germany, wolfgang.marquardt@avt.rwth-aachen.de

Abstract

Hybrid separation processes can offer significant cost-savings over simple distillation processes for close-boiling mixtures. In addition, the separation boundaries of azeotropic mixtures can be overcome. The application of hybrid processes in industry, however, is hindered by the lack of robust and efficient process synthesis tools and methods for these complex and highly integrated processes. In this work, we review an optimization-based framework composed of shortcut and rigorous design steps for the robust and efficient synthesis of separation processes. This synthesis framework is illustrated by an industrial case study for the optimal design of a hybrid process separating a ternary mixture of close-boiling isomers. A multitude of hybrid processes composed of distillation and melt crystallization units are evaluated with powerful shortcut models. A selection of promising process variants is subsequently rigorously optimized by an economic objective function and discrete-continuous optimization techniques. It is shown that the design of the cost-optimal hybrid process within the systematic synthesis framework can be accomplished with paramount robustness and efficiency.

Keywords: Process synthesis, hybrid process, shortcut method, rigorous optimization, melt crystallization

1. Introduction

Large-scale purification of reaction products in a chemical plant is typically accomplished through distillation. Innovative hybrid processes offer significant cost savings particularly for azeotropic or close-boiling mixtures and allow the cost-efficient synthesis of new products. Hybrid separation processes are characterized by the combination of two or more different unit operations, which contribute to the separation task by different physical separation principles such that separation boundaries or inefficiencies of a single unit operation can be overcome.

Despite of the inherent advantages of hybrid separation processes, they are not systematically exploited in industrial applications. A major reason is rooted in the complexity of the synthesis of these highly integrated processes. The combination of unit operations leads to a multitude of structural and operative degrees of freedom, i.e. a multitude of alternative process variants, which have to be evaluated in order to identify feasible and cost-effective variants. Considering that the operating points of structurally different process variants have to be optimized for a meaningful comparison, it is clear that the design process can be very complex and time consuming. Process design in industrial practice is usually conducted by tedious simulation studies which require detailed design specifications in an early design phase. Guided by heuristics, like those of Douglas¹, these iterative solution procedures result in a high manual effort and, in addition, no guarantee concerning the quality of the solution can be given.

2. A framework for the optimization-based design of hybrid separation processes

In order to achieve a systematic and optimization-based design procedure, a process synthesis framework for the efficient and robust design of separation processes has been developed in our previous research work²⁻³. The process synthesis framework combines shortcut methods for the conceptual design phase with rigorous optimization methods for a more detailed design. With this combination of synthesis methods of increasing level of detail, separation processes for azeotropic multicomponent mixtures can be efficiently evaluated on the basis of rigorous thermodynamics and the optimal flowsheet, the optimal process operating point and the optimal specifications (such as number of stages, location of feeds, and equipment dimensions) can be determined.

In the first step of the synthesis framework, possible flowsheet alternatives are generated (at this point) manually based on an analysis of the mixture topology. In the next step, all flowsheet variants

are evaluated successively with respect to feasibility and key indicators for cost-effectiveness such as the minimum energy demand. This procedure can be accomplished robustly and efficiently with the help of powerful shortcut methods for multicomponent mixtures based on rigorous thermodynamics like the rectification body method (RBM, see Section 4.2) for distillation. Since fully algorithmic shortcut methods and algorithmic descriptions of separation boundaries (e.g. pinch distillation boundaries for distillation⁴) are preferred, the optimization of the process operating points can be achieved robustly and efficiently. The most promising flowsheet variants can then be rigorously modeled and optimized for cost in the third step with the help of bounds and initial values from the previous shortcut evaluation. By minimizing a cost function containing capital and operating costs the rigorous optimization step provides information about the optimal flowsheet operating point as well as the number of stages and the optimal feed stage locations of staged unit operations. Since these design variables are discrete variables while the energy duties, flowrates and compositions are continuous variables, a mixed-integer nonlinear optimization problem (MINLP) has to be solved. Considering the large scale and complexity of hybrid separation processes and the nonlinearity of the underlying nonideal thermodynamics, it is obvious that these MINLP problems are particularly hard to solve. In our previous works^{3,5}, the robust and efficient solution of these MINLP problems is achieved by a favorable initialization strategy based on the results of the preceding shortcut evaluation and a reformulation as a purely continuous problem.

3. Case study: Separation of isomers

The proposed process synthesis framework is illustrated by an industrial case study, where a ternary mixture of close-boiling ortho- (o), meta- (m), and para- (p) isomers is separated into pure products by a hybrid process of melt crystallization and distillation. Although the separation of the ternary mixture by distillation is not hindered by azeotropic behavior, the close-boiling nature results in a high energy demand for a simple distillation setup. On the other hand, the mixture cannot be separated by crystallization alone because of eutectic troughs, which divide the system in three crystallization regions (c.f. Fig. 2). An efficient separation can be achieved, however, when distillation units are combined with crystallization units in a hybrid separation process. Certainly, there is a multitude of alternative process variants, i.e. combinations of crystallization and distillation units, to perform the separation task. By allowing a maximum of four separation units, one can come up with 19 feasible process variants for a feed of 66% para-, 33% ortho- and less than 1% meta-isomer as given in Fig. 1. In the following, we will show that the process variant with the lowest total annualized cost can be identified robustly and efficiently with the help of shortcut and rigorous evaluation steps of the optimization-based synthesis framework.

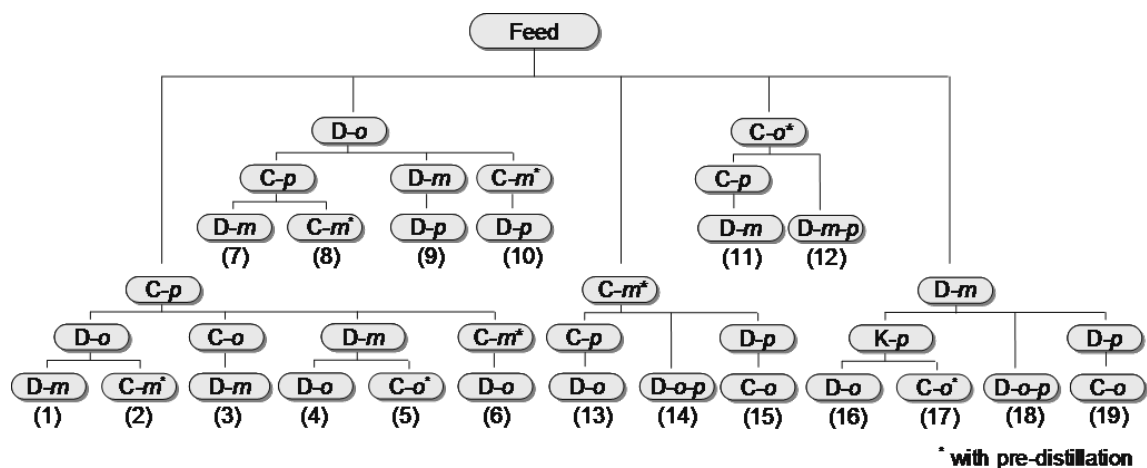


Figure 1. Tree of process variants with a maximum of four separation units (from Wallert⁶)

Note that this industrial case study of isomer separation has already been studied by Wallert⁶ and Franke et al.⁷⁻⁸. The work by Wallert is confined to a screening of process variants with shortcut methods; rigorous discrete-continuous process optimization has not been addressed. In addition, Wallert resorts to an enumeration of crystallization cascade configurations (number of stages and feed stage location) in the shortcut evaluation due to a lack of robust and reliable optimization techniques at the time. Franke et al. presented a comprehensive work on this case study, considering both shortcut evaluation and rigorous optimization. In the conceptual design step, however, these authors use simple shortcut methods, which cannot account for nonideal behavior of the crystallization tasks. The

rigorous optimization problems are then solved by a modified outer approximation algorithm which demands a large number of MINLP/NLP iterations to obtain a solution.

The work presented in this paper builds on the excellent works by Wallert⁶ and Franke et al.⁷⁻⁸ but applies recent, powerful shortcut and rigorous optimization models to achieve an optimization-based process synthesis with paramount efficiency, robustness and reliability. The optimization problems of the shortcut and rigorous design steps are solved in GAMS 22.7 on a 2.66 GHz PC.

4. Shortcut evaluation of process variants

In order to guarantee an accurate ranking of process variants in the shortcut evaluation step, we use powerful shortcut methods for distillation and crystallization which account for the non-ideality of the separation tasks. In addition, the shortcut models are fully algorithmic such that the process variants can be optimized and compared at the optimal operating point in the optimization-based evaluation.

4.1. Crystallization shortcut model

In each crystallization region, one pure isomer crystallizes as product when the temperature is lowered in the crystallizer. The configuration of the crystallizing isomer depends on the crystallization region in which the feed is located. When the temperature is further lowered, the remaining melt reaches a composition on a eutectic trough. The crystallization is stopped then, since a further decrease of the temperature would result in the crystallization of an undesired mix of isomers. The compositions and temperatures along the eutectic troughs can be calculated by

$$x_{e,i}^C \gamma_{e,i}^C = \exp\left(\frac{\Delta H_{m,i}}{R} \left(\frac{1}{T_{m,i}^C} - \frac{1}{T_e^C}\right)\right), \quad 1 = \sum_j x_{e,j}^C, \quad e = 1, \dots, 3, \quad i \in I_e \subset I. \quad (1)$$

I_e are the sets of the two isomers of the binary eutectic points where the respective eutectic troughs originate. The liquid phase activity coefficients $\gamma_{e,i}^C$ are determined by the UNIQUAC model with binary parameters adapted to solid-liquid equilibrium data.

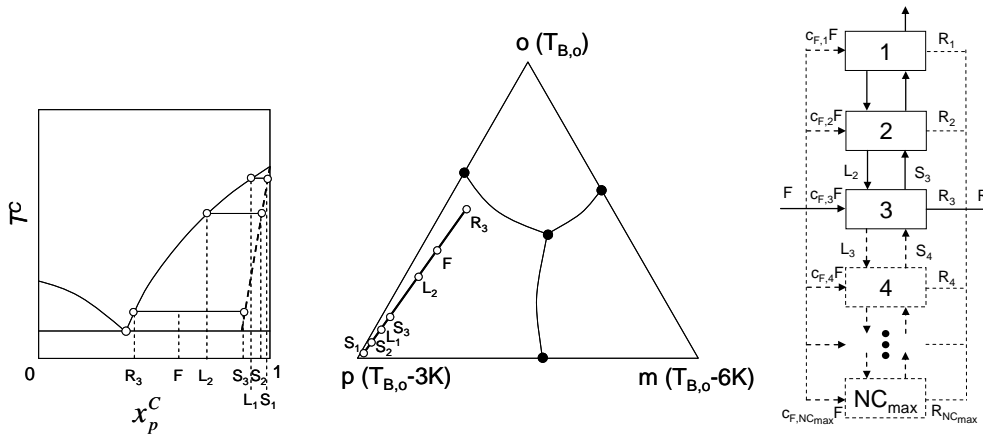


Figure 2. Non-ideal melt crystallization of isomers: temperature-concentration diagram (left), ternary phase diagram (middle, with boiling points), and crystallization cascade superstructure (right)

Franke et al.⁷⁻⁸ assume ideal conditions for the crystallization shortcut model such that the separation of a pure isomer from the remaining melt at eutectic composition can be accomplished in one crystallization stage. Industrial crystallization processes, however, never operate at ideal conditions due to inclusions of impurities in the solid phase. Thus, melt crystallization processes are carried out as staged processes where the liquid and solid phases are exchanged between stages in a counter-current pattern. The energy demand of such a staged process exceeds the energy demand of an ideal, single-staged process by a multitude, e.g. by a factor larger than 5.5 for the crystallization tasks separating the p-isomer in the case study. We therefore chose to model the crystallization shortcut as a nonideal staged process similar to Wallert⁶. In contrast to distillation however, where the energy demand decreases monotonously with the number of stages, crystallization processes exhibit a clear minimum energy demand at an optimal number of stages and an optimal location of the feed stage. It is therefore essential to optimize these discrete design variables in the shortcut step in order to

facilitate an accurate evaluation of the minimum energy demand. Wallert formulates this discrete-continuous optimization problem as a general disjunctive programming (GDP) problem⁹, where Boolean operators model the existence of stages. The GDP problem is then reformulated as a MINLP problem with the help of big-M constraints. Wallert reports that the optimization by a branch & bound solver leads to longer solution times than a simple enumeration of the discrete variables for a maximum number of six stages. While the enumeration of discrete variables may be feasible for a single crystallization unit, it is clear that hybrid processes with several crystallization units, distillation units, or other unit operations can only be optimized efficiently by powerful optimization algorithms. The formulation of the crystallization cascade optimization problem with Boolean variables for the existence of stages in a GDP yields a very disjunct optimization problem. As a consequence, the reformulation with big-M constraints results in a loose relaxation and long computational times for the solution with MINLP solvers. We have therefore used a very tight MINLP superstructure for the optimization of crystallization stages instead (c.f. Fig. 2, right), which is similar to the superstructure for distillation column optimization used in this and our earlier work³. Specifically, the number of crystallization stages is modeled by a variable draw of residue melt on each stage and a variable feed. Using this tight superstructure, the variable crystallization cascade structure actually takes on a discrete number of stages at the local minima of the energy demand. A distributed residue melt draw leads to reduced liquid and solid streams in the cascade behind the first partial residue melt draw. This implies a reduced separation driving force and a penalty on the energy demand for the cascade. As a consequence, additional measures to force discrete solutions are not necessary. The crystallization cascade model is given by the following equations (see also Wallert⁶):

$$0 = c_{F,nc}^C F^C + S_{nc+1}^C + L_{nc-1}^C - S_{nc}^C - L_{nc}^C - R_M^C, \quad nc \in NC, \quad (2)$$

$$0 = c_{F,nc}^C F^C x_{F,i}^C + S_{nc+1}^C z_{nc+1,i}^C + L_{nc-1}^C x_{nc-1,i}^C - S_{nc}^C z_{nc,i}^C - L_{nc}^C x_{nc,i}^C - R_M^C x_{nc,i}^C, \quad nc \in NC, i \in I, \quad (3)$$

$$0 = \sum_i z_{nc,i}^C, \quad 1 = \sum_i x_{nc,i}^C, \quad 1 = \sum_i x_{F,i}^C, \quad 0 \leq c_{F,nc}^C \leq 1, \quad 1 = \sum_{nc} c_{F,nc}^C, \quad nc \in NC, \quad (4)$$

$$0 = (T_{m,ic}^C - T_{nc}^C) - M(1 - z_{nc,ic}^C), \quad nc \in NC, \quad (5)$$

$$0 = \frac{x_{nc,i \neq j,ic}^C}{x_{F,i \neq j,ic}^C} - \frac{x_{nc,j \neq i,ic}^C}{x_{F,j \neq i,ic}^C}, \quad nc \in NC, \quad i, j \in I, \quad (6)$$

$$0 = x_{nc,ic}^C \gamma_{nc,ic}^C - \exp\left(\frac{\Delta H_{m,ic}}{R} \left(\frac{1}{T_{m,ic}^C} - \frac{1}{T_{nc}^C}\right)\right), \quad nc \in NC, \quad (7)$$

$$r_{f,min} \leq \frac{S_{nc}^C}{S_{nc}^C + L_{nc}^C} \leq r_{f,max}, \quad nc \in NC, \quad (8)$$

$$0 = \frac{x_{e,i \neq j,ic}^C}{x_{F,i \neq j,ic}^C} - \frac{x_{e,j \neq i,ic}^C}{x_{F,j \neq i,ic}^C}, \quad i, j \in I, \quad x_{nc,ic}^C \geq x_{e,ic}^C, \quad e = 1, \dots, 3, \quad (9)$$

$$Q^C = 4 \cdot K \cdot S_1^C \Delta H_{m,ic}, \quad K = \frac{\sum_{nc} S_{nc}^C}{S_1^C}. \quad (10)$$

Eq. (2) and (3) are the total and the component mass balances. Eq. (4) provides closure conditions for concentrations and feed distribution. Based on the results of Matsuoka et al.¹⁰, Eq. (5) models the non-ideality of the crystallization, i.e. the impurities in the crystal layer, by a linear correlation between temperature in the crystallizer and composition of the crystal layer (c.f. Fig. 2, left). Together with Eq. (6), which defines the ratio of the isomers in the melt, we obtain the condition that all liquid and solid compositions are located on a line through the feed composition and the pure isomer vertex (c.f. Fig. 2, middle). The melt compositions on the stages are related to the crystallization temperatures by eq. (7). Again, the liquid activity coefficients are calculated by the UNIQUAC model with binary parameters adapted to solid-liquid equilibrium data. Eq. (8) constrains the freezing ratio of a crystallization stage between lower and upper bounds to ensure a feasible operation. Eqs. (9) together with eq. (1) guarantees that the compositions of the melt are located in the appropriate crystallization region. The energy demand of the crystallization cascade is estimated by eq. (10) of Wellinghoff and Wintermantel¹¹. Here, K is the crystallization effort, defined as the ratio of the total amount of crystals produced to the amount of solid product S_1^C , which accounts for the existence of more than one stage, i.e. the non-ideality of the crystallization. The required energy for cooling the apparatus and pumping the liquor is considered by Wellinghoff and Wintermantel with the factor 4 in eq. (10). Note that

additional to the cooling duty, the same amount of energy (minus the heat induced by the pump) is needed for heating the apparatus and melting the crystal layers.

4.2. Distillation shortcut model

Wallert⁶ uses the rectification body method (RBM)¹² for the estimation of the minimum energy demand of the distillation tasks in the hybrid processes. The RBM is a pinch-based and algorithmically accessible shortcut method for the determination of the minimum energy demand of multicomponent, nonideal distillation. Specifically, the RBM first identifies all pinch points and classifies the relevant pinches for the separation. Here, possible paths along pinch points with an increasing number of stable eigenvectors are generated and checked for thermodynamic consistency by excluding paths, where the entropy production does not increase strictly monotonously. Linear rectification bodies which approximately describe the manifold of all profiles are then constructed for each section by linearly connecting the pinch points contained in the paths. The minimum energy demand is calculated by iteratively identifying the lowest reboiler duty that results in an intersection of a set of bodies.

In this work, we calculate the distillation shortcuts with the feed angle method (FAM)¹³, which is a refinement of the RBM. The FAM uses the relevant pinch points identified by an initialization with the RBM and calculates one tray above or below the feed pinch in the non-pinch column section. For the determination of the minimum energy demand, the composition vector constructed by the feed pinch and the calculated tray has to point towards the relevant saddle pinch point in the non-pinch column section. Compared to the RBM, the FAM is better suited for application in an optimization-based flowsheet evaluation because it does not identify and classify possible pinch points in every iteration step of the flowsheet optimization algorithm. In addition, the FAM can be more accurate for highly nonideal mixtures as it includes the information of one distillation tray at the feed pinch. It needs to be mentioned, however, that the FAM needs to be initialized by the RBM to obtain information about the relevant pinch points.

4.3. Screening of process variants with shortcut methods

We use the shortcut methods for distillation and crystallization as described in Sections 4.1 and 4.2 for the evaluation of the process variants shown in Fig. 1. During the design process, the operating pressure of the distillation tasks is fixed at a value which allows the use of low pressure steam as hot utility. Impurity bounds were added to the intermediate distillation products in the shortcut evaluation step. These impurity bounds prohibit sharp splits, which lead to high numbers of trays and expensive capital costs for the distillation tasks in the rigorous optimization step. The impurity bounds were set to 0.2 for the o- and p-isomers and 0.1 for the m-isomer. The intermediate distillate products which are fed into another distillation column are not condensed but transferred as saturated vapor as a measure of heat integration.

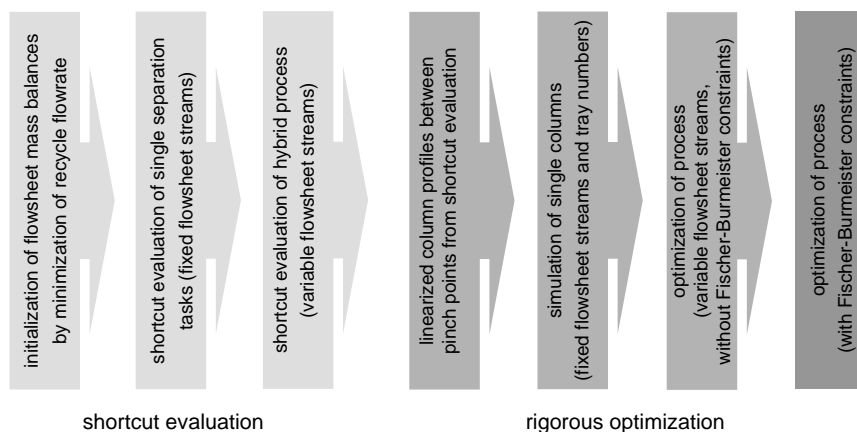


Figure 3. Initialization procedures of shortcut evaluation and rigorous optimization

A meaningful evaluation of different flowsheet variants can only be achieved when the processes are compared at their respective optimal operating point. Hence, the degrees of freedom on the flowsheet level, i.e. the flowrates and compositions of the intermediate and recycle streams need to be optimized together with the structural decisions for the crystallization cascades (c.f. section 4.1). In order to achieve a robust, efficient and reliable solution of this nonlinear optimization problem, a favorable initialization strategy is of paramount importance, the more so due to the coupling of different unit

operations in the hybrid processes. The initialization procedure applied in this case study is carried out in several steps as shown in Fig. 3. In our experience, a stepwise initialization of the shortcut evaluation problem helps both robustness as well as efficiency, although more problems have to be solved.

In the first step of the initialization, the flowsheet mass balances are initialized at the minimum recycle flowrate. For this purpose, a nonlinear programming (NLP) problem is solved, where the recycle flowrate is minimized such that the flowsheet mass balances, the purity and impurity constraints, and the limitations by eutectic troughs are fulfilled. In the next initialization step, the flowrates and compositions of the flowsheet streams are fixed at the values of the preceding step and all separation units are evaluated by their respective shortcut method to initialize the shortcut model equations. In the final step, the fixed flowsheet variables are released such that the minimum energy demand of the hybrid process can be determined by solving a NLP problem. Here, the objective function is the minimization of a weighted sum of the energy duties of the hybrid process. The weights are introduced, since heating and cooling utilities of different costs are compared. Wallert⁶ and Franke et al.⁷⁻⁸ consider the heating duties of the distillation units and only the cooling duties of the crystallization units. In our work, we additionally included the heating duties for the melting of the crystal layers as suggested by Wellinghoff and Wintermantel¹¹, since the low pressure steam required for these heating duties contributes significantly to the overall energy costs. The objective function is constrained by the product purities, the impurity constraints for the intermediate distillate products, the flowsheet mass balances and the shortcut models of the unit operations. The optimization variables are the independent flowsheet variables and the number of stages and feed stage locations of the crystallization cascades.

Table 1. Energy duties for a selection of process variants

process	1	16	13	6	9	18	7	3	11
$Q_{\text{tot}}/Q_{\text{tot, min}}$	1	1.0007	1.0008	1.045	1.098	1.222	1.239	1.391	1.432

The solution times for the shortcut evaluation of one hybrid process including the initialization procedure takes about 15 seconds on average. The optimized energy duties for a selection of process variants are shown in Table 1. It can be seen that the pure distillation process (process 9) requires only 10% more energy than the best hybrid process. The pure distillation processes benefit most from the heat integration by transfer of distillate streams as vapor. Furthermore, it needs to be noted that the constraints for impurities in the intermediate distillate products, i.e. the constraints for sloppy distillation splits, were dropped for the pure distillation processes. The capital costs of the high numbers of column trays for sharp splits will show in the rigorous optimization (c.f. section 5.3).

5. Rigorous optimization models

Following the process synthesis framework, a selection of the most promising process variants is further evaluated in the rigorous optimization step. Here, the total annualized costs consisting of operating and capital costs are minimized to identify the cost-optimal process variant.

5.1. Rigorous melt crystallization model

The rigorous crystallization model is based on the shortcut crystallization model. The cascade superstructure of Fig. 2 is reused, as are the model equations (1)-(10). We add correlations for the dimensioning and costing of the apparatus, which are taken from Wallert⁶. The capital costs of the crystallization cascade are composed of the costs for one shell and tube heat exchanger and for NC surge drums. Even with the addition of the capital costs, the variable crystallization cascade structure still takes on a discrete number of stages at the local minima of the total cost function. A distributed residue melt draw implies a penalty on the energy demand and the total cost as explained in Section 4.1 and, thus, binary variables to model the existence of stages as in Franke⁷⁻⁸ is not necessary.

5.2. Rigorous distillation model

The rigorous optimization step provides information about the optimal number of column trays and the optimal feed tray locations. Since these design variables are discrete variables while the energy duties, flowrates and compositions are continuous variables, a discrete-continuous rigorous column model was formulated. This model is adopted from our earlier work on the optimization of multicolumn distillation processes³. The number of active column trays is modeled by a variable location of reflux and the reboil trays. Comparably to our earlier works, the robust and efficient solution of the discrete-continuous problem is achieved by a reformulation as a purely continuous problem and a favorable

initialization strategy based on the results of the preceding shortcut evaluation. For the continuous reformulation of the problem, the discrete variables are replaced by continuous decision variables. Discrete solutions are reached by the addition of special nonlinear constraints in the form of the Fischer-Burmeister functions, which force the continuous decision variables c_{nd}^D to discrete values:

$$0 = 1 - \sqrt{(c_{nd}^D)^2 + (1 - c_{nd}^D)^2}, \quad nd \in ND. \quad (11)$$

5.3. Rigorous optimization of selected variants

Before an entire hybrid process is rigorously optimized, the rigorous distillation column models are initialized separately for each column at the fixed flowsheet operating point determined in the shortcut evaluation step. This initialization procedure is shown in Fig. 3 (right). At first, linear column composition and temperature profiles are derived from the linear piece-wise combination of the pinch points calculated by the FAM in the shortcut step to provide very good approximations of the actual column profiles. These linear profiles then serve as initialization for a rigorous column simulation for which the tray number is fixed at a user-specified maximum value and the relaxed feed tray location variable is optimized by a minimization of the reboiler duty to provide excellent initial values for the rigorous tray optimization.

Finally, the rigorous distillation and crystallization models are connected by the flowsheet streams. We release the previously fixed flowsheet operating point as well as the distillation tray numbers. We solve this problem without the highly nonlinear Fischer-Burmeister constraints (eq. (11)) initially, such that the decision variables of the distillation columns (feed locations and reflux as well as reboil locations) are optimally distributed among some column trays and the problem converges reliably to favorable solution regions. Due to the tight distillation column superstructure, some relaxed decision variables converge to integer values in the local optima even without being constrained to integrality. The remaining relaxed discrete variables exhibit a very narrow distribution among a few neighboring trays. As discussed in section 4.1, this is also true for the discrete decisions of the crystallization cascade structure. In the final solution step, the Fischer-Burmeister constraints (eq. (11)) are activated in order to guarantee optimal integer values for all discrete variables.

Table 2. Total annualized costs for the three hybrid processes and one pure distillation process

process	TAC _{tot} /TAC _{tot,min}	TAC _{D1} /TAC _{tot,min}	TAC _{D2} /TAC _{tot,min}	TAC _{C1} /TAC _{tot,min}	TAC _{C2} /TAC _{tot,min}
6	1	0.046	0.458	0.485	0.011
1	1.01	0.462	0.063	0.485	-
16	1.02	0.065	0.466	0.489	-
9	1.95	1.225	0.728	-	-

The total annualized costs for the three most cost-efficient hybrid processes (1,6,16) and the best pure distillation process are given in Table 2. All three hybrid processes separate the medium boiling p-isomer via crystallization. Process 6 contains two crystallization units and exhibits the lowest total annual costs despite slightly higher energy demand in the shortcut evaluation compared two processes 1 and 16. The pure distillation process (process 9) costs almost twice as much as the hybrid processes, mostly due to the large number of trays required for the sharp splits.

Contrary to the heat integration in the shortcut evaluation, all intermediate distillate products are condensed and transferred as saturated liquid to subsequent distillation columns. Saturated liquid feeds yielded significantly smaller vapor flows in the column than vapor feeds. The resulting smaller diameters and lower capital costs for the distillation columns more than compensated for the larger energy duties compared to vapor feeds.

The optimal numbers of stages, locations of feed stages, and flowsheet mass balances of process 6 are shown in Fig. 4. Note that the distillation units perform sloppy splits in the optimal solution although the impurity constraints of the shortcut evaluation are dropped in the rigorous optimization.

Thanks to the favorable initialization procedure we were able to solve the rigorous optimization problems robustly and obtained good local optima. Furthermore, the tight continuous formulation of the crystallization model together with the continuous reformulation of the distillation column model allowed us two find an optimal discrete solution by solving only two NLP problems plus the initialization for each hybrid process. Accordingly, the computational time of the rigorous optimization of process 6 with 320 discrete and about 3000 continuous variables amounted to only 112 seconds, including the initialization phase. Such computational efficiency for the discrete-continuous optimization of a large-scale process cannot be reached by solving a MINLP problem with the common outer-approximation or branch & bounds solvers, which rely on a MILP/NLP iteration or tree search procedure, respectively. Franke et al.⁷⁻⁸ achieve a robust and reliable performance for the rigorous MINLP optimization of the hybrid processes in this case study with the help of a modified

outer approximation solver. Still, they report 66 NLP and 59 MILP iteration steps for the rigorous optimization of one hybrid process.

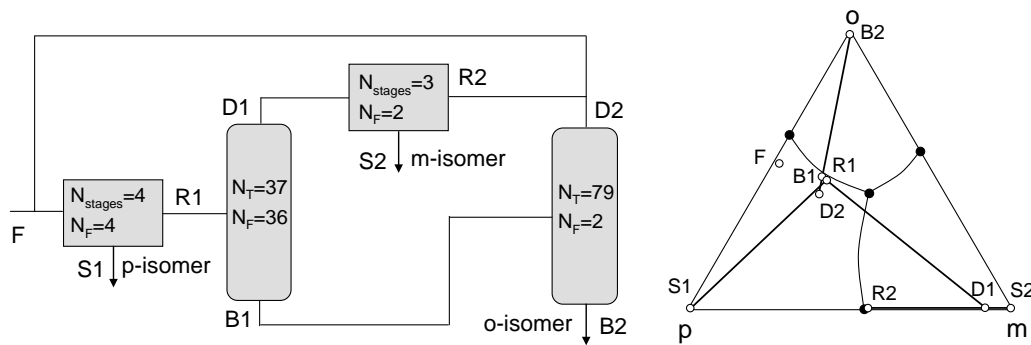


Figure 4. Numbers of stages, feed stage locations, and flowsheet mass balances of process 6

6. Conclusions

We have presented a stepwise synthesis framework for the optimization-based design of cost optimal, hybrid separation processes. The framework is illustrated by an industrial case study, where a ternary mixture of close-boiling ortho- (o), meta- (m), and para- (p) isomers is separated into pure products by a hybrid process of melt crystallization and distillation. In a first design step, powerful shortcut methods accounting for the nonidealities of the unit operations are used to evaluate alternative flowsheet variants. A selection of the most promising variants is then rigorously optimized in the second design step in order to identify the most cost-efficient flowsheet and obtain detailed unit specifications. The benefit of our approach lies in the ability to deal with complex hybrid flowsheets and design the optimal process with paramount robustness and efficiency. The rigorous optimization of a large-scale hybrid process can be achieved in a few CPU minutes due to the initialization provided by the shortcut evaluation and the continuous reformulation of the MINLP problem.

Acknowledgements

The authors would like to acknowledge financial support by the cluster of excellence “Tailor Made Fuels from Biomass”.

Notation

c	decision variable	r_f	freezing ratio	Subscripts	
F	feed stream [mol/s]	R_M	residue melt [mol/s]	F	feed
γ	activity coefficient	S	solid stream [mols/s]	i, j	index for component
ΔH_m	melt enthalpy [J/mol]	T	temperature [K]	ic	crystallizing component
K	crystallization effort	T_m	melting temperature [K]	nc	index for stage
L	liquid stream [mol/s]	x	liquid composition	Superscripts	
M	constant of proportionality	z	solid composition	C	crystallization
Q	energy duty [W]				
R	gas constant [J/K/mol]				

References

1. J.M. Douglas, *Conceptual Design of Chemical Processes*, McGraw-Hill (1988)
2. W. Marquardt et al., *Chin. J. Chem. Eng.*, 16(2008) 333
3. K. Kraemer et al., *Ind. Eng. Chem. Res.*, 48(2009) 6749-6764
4. A.G. Davydian et al., *Theor. Found. Chem. Eng.*, 4(1997) 327-338
5. S. Kossack et al., *Ind. Eng. Chem. Res.*, 45(2006) 8492
6. C. Wallert, *Konzeptioneller Entwurf und wirtschaftliche Bewertung hybrider Trennprozesse mit Näherungsverfahren*, VDI Verlag (2008)
7. M. Franke et al., *AIChE J.*, 54(2008) 2925-2942
8. M. Franke, *Optimierung hybrider Verfahren*, VDI Verlag (2006)
9. R. Raman and I.E. Grossmann, *Comput. Chem. Eng.*, 18(1993) 563-578
10. M. Matsuoka et al., *J. Chem. Eng. Jpn.*, 19(1986) 181-185
11. G. Wellinghof and K. Wintermantel, *Chem. Ing. Tech.*, 63(1991) 881-891
12. J. Bausa et al., *AIChE J.*, 44(1998) 2181-2198
13. K. Kraemer et al., submitted to: Distillation Absorption 2010, Eindhoven, Netherlands